Stability of Data-Driven Predictive Control for Nonlinear Systems via Koopman Embeddings

Amin Taghieh and SangWoo Park

***Abstract*— Data-driven model predictive control (MPC) based on Willems' fundamental lemma has proven effective for linear systems, but extending its stability guarantees to nonlinear systems remains an open challenge. In this paper, we establish conditions under which data-driven MPC, applied directly to input-output data from a nonlinear system, yields practical exponential stability. The key insight is that the existence of an approximate Koopman linear embedding lets the nonlinear data be interpreted as noisy data from a linear time-invariant system, bringing the problem within the scope of existing robust data-driven MPC theory. Crucially, the embedding serves only as a theoretical certificate: the controller operates on raw nonlinear data without using the lifting functions. We further show that the proportional structure of the Koopman residual yields an asymptotic bound determined by the offset c_0 of the embedding error rather than by its worst-case magnitude over the operating region. The framework is demonstrated on a synchronous generator connected to an infinite bus, for which we construct an explicit physics-informed embedding with error bounds.**

***Index Terms*— Data-driven control, Stability of nonlinear systems, Predictive control for nonlinear systems**

I. Introduction

A. Motivation and Background

DATA-DRIVEN control methods that bypass explicit system identification have become a central topic in modern control theory, building on Willems' fundamental lemma [1]. For linear time-invariant (LTI) systems, this lemma provides a complete, non-parametric characterization of the system's trajectory space using a single persistently exciting input-output trajectory. When combined with model predictive control (MPC), this yields the Data-Enabled Predictive Control (DeePC) algorithm [2] and its variants with rigorous closed-loop stability and robustness guarantees [3].

Beyond MPC, Willems' fundamental lemma has enabled a broad range of data-driven designs for LTI systems [4]–[6], providing a mature foundation that nonetheless relies fundamentally on linearity: the data must come from a linear system, possibly noise-corrupted. Several approaches extend data-driven methods to specific nonlinear classes: LTI embeddings for bilinear systems [7], sum-of-squares programs for polynomial systems [8], coordinate transformations for feedback-linearizable systems [9], and linearization-based tracking MPC [10].

A different perspective is offered by Koopman operator theory [11], which provides a pathway toward applying linear methods to broad classes of nonlinear systems by lifting the dynamics into a higher-dimensional (potentially infinite) functional space where they evolve linearly. This Koopman-based idea has been pursued along two distinct lines. The first is *identification-based*: one learns a finite-dimensional Koopman model from data via extended dynamic mode decomposition (EDMD) [12] and then applies standard MPC using the identified model. Recent work has established stability guarantees for this approach under proportional approximation error bounds [13], [14]. The second line is *directly data-driven*: the extended Willems' fundamental lemma of [15] shows that the trajectory space of a nonlinear system admitting an exact Koopman embedding can be represented directly from nonlinear data without knowledge of the lifting functions.

However, a critical subtlety is that *exact* finite-dimensional Koopman embeddings rarely exist for physical systems. For example, systems with trigonometric nonlinearities or bilinear terms generically require infinite-dimensional embeddings to achieve exact closure of the observables. Therefore, a fundamental question remains: under what conditions is the resulting closed loop stable, and how does the stability margin depend on the system's deviation from linearity? This makes the *approximate* embedding framework not merely a theoretical convenience, but a practical necessity. Because a finite-dimensional embedding can only be expected to hold on a bounded region, the guarantees we obtain are inherently *local*, certifying the equilibrium whose basin contains the operating region; this is the natural setting for nonlinear systems, which may possess multiple disconnected equilibria.

In this paper, we establish rigorous conditions under which data-driven MPC, applied directly to input-output data from a nonlinear system, yields practical exponential stability. The key insight is that the existence of an approximate Koopman linear embedding certifies that the nonlinear data can be interpreted as noisy data from a linear time-invariant system, enabling the application of existing robust stability theories. Our contributions are as follows: (i) We formalize the notion of an *approximate Koopman linear embedding with proportional-with-offset error bounds*; (ii) We prove that the robust data-driven MPC scheme of [3], applied directly to input-output data from a nonlinear system, yields practical exponential stability whenever the system admits an approximate Koopman embedding with sufficiently small error; unlike indirect data-driven Koopman methods [13], [14], [16] that embed an identified surrogate inside the controller, our scheme is directly data-driven and uses the embedding only as an analytical certificate, with no online evaluation of the lifting; (iii) We

The authors are with the New Jersey Institute of Technology, Newark, NJ 07102 USA. (e-mails: at2228@njit.edu, sangwoo.park@njit.edu)

provide a rigorous bridge between the Koopman approximation error and the bounded noise framework of [3], showing how the nonlinearity gap maps to an effective noise level $\bar{\epsilon}$ that determines the stability margin; (iv) As a representative application, we construct an approximate Koopman embedding for a third-order synchronous generator connected to an infinite bus, with quantified error bounds, and verify the framework's effectiveness.

B. Notation

For a vector x and positive definite matrix P, a weighted norm is defined as $\|x\|_P := \sqrt{x^\top P x}$. We write $\mathrm{col}(\cdot)$ for column stacking and $x_{[a,b]} := \mathrm{col}(x_a, \dots, x_b)$. For a signal $\{x_k\}_{k=0}^{N-1} \subset \mathbb{R}^q$, the Hankel matrix of depth L is $\mathcal{H}_L(x) := \begin{bmatrix} x_{[0,L-1]} & x_{[1,L]} & \cdots & x_{[N-L,N-1]} \end{bmatrix} \in \mathbb{R}^{qL\times(N-L+1)}$, whose columns are the length-L windows of the signal. A sequence $\{x_k\}_{k=0}^{N-1} \subset \mathbb{R}^q$ is *persistently exciting (PE)* of order L if $\mathrm{rank}(\mathcal{H}_L(x)) = qL$.

II. Approximate Koopman Embedding

A. Koopman Linear Embedding

We consider a discrete-time nonlinear time-invariant system

$$x_{k+1} = f(x_k, u_k), \quad y_k = g(x_k, u_k) \tag{1}$$

with state $x_k \in \mathbb{R}^n$, input $u_k \in \mathbb{R}^m$, and output $y_k \in \mathbb{R}^p$. We assume the existence of an equilibrium $(x_s, u_s) \in \mathbb{R}^n \times \mathbb{R}^m$ satisfying $x_s = f(x_s, u_s)$ and $y_s = g(x_s, u_s)$, around which we define the deviation variables $\bar{x}_k := x_k - x_s$, $\bar{u}_k := u_k - u_s$, $\bar{y}_k := y_k - y_s$, and, given a lifting $\Phi = (\Phi_1, \dots, \Phi_{n_z})^\top : \mathbb{R}^n \to \mathbb{R}^{n_z}$ with linearly independent components, $\bar{z}_k := \Phi(x_k) - \Phi(x_s)$. Throughout, we assume that the system operates in a compact domain $\mathcal{X} \subset \mathbb{R}^n$ containing x_s in its interior, with input constrained to a compact set $\mathcal{U} \subset \mathbb{R}^m$ containing u_s in its interior.

Definition 1 (Koopman Linear Embedding [15])**.** The nonlinear system (1) admits a Koopman linear embedding of dimension n_z if there exist Φ, A, B, C, D such that $\bar{z}_k$ satisfies

$$\bar{z}_{k+1} = A\bar{z}_k + B\bar{u}_k, \quad \bar{y}_k = C\bar{z}_k + D\bar{u}_k \tag{2}$$

along all trajectories of (1) within the operating domain $\mathcal{X}$, with $A \in \mathbb{R}^{n_z\times n_z}$, $B \in \mathbb{R}^{n_z\times m}$, $C \in \mathbb{R}^{p\times n_z}$, $D \in \mathbb{R}^{p\times m}$. Evaluating (2) at the equilibrium ($\bar{z}_k = 0$, $\bar{u}_k = 0$) yields the consistency identities $\Phi(x_s) = A\Phi(x_s) + Bu_s$ and $y_s = C\Phi(x_s) + Du_s$, which hold automatically.

Definition 2 (Approximate Koopman Embedding)**.** The system (1) admits an *approximate Koopman linear embedding* with *proportional error bound* $(\epsilon_A, \epsilon_B, \epsilon_C)$ and *offset* $c_0 \geq 0$ if there exist Φ, A, B, C, D such that $\bar{z}_k$ satisfies

$$\bar{z}_{k+1} = A\bar{z}_k + B\bar{u}_k + e_k, \quad \bar{y}_k = C\bar{z}_k + D\bar{u}_k + \eta_k \tag{3}$$

along all trajectories within $\mathcal{X}$, where the residuals satisfy:

$$\|e_k\|_2 \leq \epsilon_A \|\bar{z}_k\|_2 + \epsilon_B \|\bar{u}_k\|_2 + c_0 \tag{4}$$

$$\|\eta_k\|_2 \leq \epsilon_C \|\bar{z}_k\|_2 \tag{5}$$

for constants $\epsilon_A, \epsilon_B, \epsilon_C \geq 0$. When $c_0 = 0$, the bound is *purely proportional*; when $c_0 > 0$, it is *proportional-with-offset*. Evaluating (3) at the equilibrium gives $\|e_s\|_2 \leq c_0$ and $\eta_s = 0$; equivalently, the consistency identity $y_s = C\Phi(x_s) + Du_s$ holds exactly, and $\|\Phi(x_s) - A\Phi(x_s) - Bu_s\|_2 \leq c_0$.

Assumption 1. The lifting $\Phi : \mathbb{R}^n \to \mathbb{R}^{n_z}$ is continuously differentiable and *bi-Lipschitz* on $\mathcal{X}$: there exist constants $\ell_\Phi, L_\Phi > 0$ such that, for all $x \in \mathcal{X}$,

$$\ell_\Phi \|x - x_s\|_2 \leq \|\Phi(x) - \Phi(x_s)\|_2 \leq L_\Phi \|x - x_s\|_2 . \tag{6}$$

The concept of proportional error bounds for data-driven Koopman surrogates was introduced by Bold et al. [17] in the EDMD setting and developed further for kernel EDMD in [13], [18], where the bounds on the full approximation error can be rigorously verified; [19] subsequently established asymptotic stability for Koopman MPC without stabilizing terminal conditions. As noted in Section I, our framework differs from these indirect methods (and from SafEDMD [16]) in that the embedding is used purely as an analytical certificate.

The centering at equilibrium in (4) is essential: a purely proportional bound ($c_0 = 0$) guarantees *exponential* stability (the error vanishes at the setpoint at an exponential rate), while a proportional-with-offset bound ($c_0 > 0$) yields *practical exponential stability* (exponential convergence to a neighborhood of radius $O(c_0)$). Definition 2 combines the exact embedding concept of [15] with the proportional error framework of [13], [14], extended to include the offset term that arises naturally in finite-dimensional approximations. Given the lifting Φ, we further define the following diameters, $\mathrm{diam}_z := \max_{x\in\mathcal{X}} \|\Phi(x) - \Phi(x_s)\|_2$ and $\mathrm{diam}_u := \max_{u\in\mathcal{U}} \|u - u_s\|_2$, both of which are finite by compactness.

Remark 1 (Interpretation of Approximate Embedding)**.** The lifting Φ is a given, fixed function, and A, B, C, D are an optimal LTI surrogate that, given Φ, minimize the lifted one-step prediction residual on the data (e.g., via EDMD [12]). The residual e_k is structural: it arises because $\Phi(f(x_k, u_k)) \neq A\Phi(x_k) + Bu_k$ in finite dimensions, i.e., the observable algebra does not close. We call the residual-free system ($e_k = \eta_k = 0$) the *nominal Koopman system*; it is a finite-dimensional linear model whose deviation from the plant is quantified by $(\epsilon_A, \epsilon_B, \epsilon_C, c_0)$, following the robust-control convention of [3].

III. Stability of Data-Driven MPC Under Approximate Koopman Embeddings

A. Data-Driven Representation

Following the *extended* Willems' fundamental lemma [15], the trajectory space of a nonlinear system admitting an exact Koopman embedding of dimension n_z admits a finite-dimensional, non-parametric data-driven representation. Specifically, given $l \geq mL + n_z$ length-L trajectories $\mathrm{col}(u^{d,i}, y^{d,i})$, $i = 1, \dots, l$, with $L = T_{\mathrm{ini}} + N$, define the lifted-excitation matrix

$$H_K := \begin{bmatrix} u^{d,1} & \cdots & u^{d,l} \\ \Phi(x_0^1) & \cdots & \Phi(x_0^l) \end{bmatrix} \in \mathbb{R}^{(mL+n_z)\times l}, \tag{7}$$

and the input-output data matrix

$$H_d := \begin{bmatrix} U_P^\top & U_F^\top & Y_P^\top & Y_F^\top \end{bmatrix}^\top \in \mathbb{R}^{(m+p)L\times l}, \tag{8}$$

where each block is built from the l trajectories: $U_P \in \mathbb{R}^{mT_{\mathrm{ini}}\times l}$ and $Y_P \in \mathbb{R}^{pT_{\mathrm{ini}}\times l}$ stack the first T_{ini} steps (the *past* window) of the input and output trajectories as columns, while $U_F \in \mathbb{R}^{mN\times l}$ and $Y_F \in \mathbb{R}^{pN\times l}$ stack the remaining N steps (the *future* window). We say the library satisfies *lifted*

excitation of order L [15] when H_K has full row rank. Under this condition and $T_{\text{ini}} \geq n_z$, [15, Thm. 3] shows that every length-L trajectory of the nonlinear system can be represented as a linear combination of the columns of H_d. Throughout, we adopt the standard sliding-window data-collection regime, in which a single offline trajectory of length T_{data} is partitioned into $l = T_{\text{data}} - L + 1$ overlapping length-L subsequences; in this regime, persistent excitation of u^d of order $L + n_z$ (along with controllability) implies lifted excitation of order L [15].

Exact Koopman embeddings rarely exist for nonlinear systems, raising the question: how does this representation degrade under an approximate embedding, and can it still support a stability-preserving controller? Our contribution is to answer this affirmatively by recasting the residuals of Definition 2 as bounded noise: e_k acts as a bounded process disturbance and η_k as bounded output noise, allowing us to view (u^d, y^d) as noisy data from the nominal LTI Koopman system. This brings the problem within the scope of robust LTI data-driven MPC, and we adopt the scheme of [3, Algorithm 2] with $T_{\text{ini}} = n_z$ so that $L = n_z + N$. The scheme requires a *noise tolerance parameter* $\bar{\epsilon} > 0$, an upper bound on the modeling noise level; Lemma 1 below derives an explicit value of $\bar{\epsilon}$ in terms of the Koopman approximation constants. With this parameter, at each discrete time step $t \in \mathbb{Z}_{\geq 0}$, the MPC solves the following optimization over the decision variables $\alpha(t) \in \mathbb{R}^l$, $\sigma(t) \in \mathbb{R}^{pL}$, $\hat{u}(t) \in \mathbb{R}^{mL}$, and $\hat{y}(t) \in \mathbb{R}^{pL}$:

$$\min_{\alpha,\sigma,\hat{u},\hat{y}} \sum_{k=0}^{L-1} \ell(\hat{u}_k(t), \hat{y}_k(t)) + \lambda_\alpha \bar{\epsilon} \|\alpha(t)\|_2^2 + \lambda_\sigma \|\sigma(t)\|_2^2 \tag{9a}$$

$$\text{s.t.} \begin{bmatrix} \hat{u}_{[0,L-1]}(t) \\ \hat{y}_{[0,L-1]}(t) \end{bmatrix} = H_d\, \alpha(t) + \begin{bmatrix} 0 \\ \sigma(t) \end{bmatrix} \tag{9b}$$

$$\hat{u}_{[0,n_z-1]}(t) = u_{[t-n_z,t-1]}, \quad \hat{y}_{[0,n_z-1]}(t) = y_{[t-n_z,t-1]} \tag{9c}$$

$$\hat{u}_{[L-n_z,L-1]}(t) = u_s^{n_z}, \quad \hat{y}_{[L-n_z,L-1]}(t) = y_s^{n_z} \tag{9d}$$

$$\hat{u}_k(t) \in \mathcal{U}, \quad \|\sigma_k(t)\|_\infty \leq \bar{\epsilon}(1 + \|\alpha(t)\|_1) \tag{9e}$$

where $\ell(\hat{u}, \hat{y}) = \|\hat{u} - u_s\|_R^2 + \|\hat{y} - y_s\|_Q^2$ with $Q, R \succ 0$, and $\lambda_\alpha, \lambda_\sigma > 0$ are regularization parameters. The vectors $u_s^{n_z} \in \mathbb{R}^{mn_z}$ and $y_s^{n_z} \in \mathbb{R}^{pn_z}$ denote n_z stacked copies of u_s and y_s, respectively. The first/last n_z steps of the length-L predictions $(\hat{u}, \hat{y})$ are constrained to match recent measurements (9c) and the equilibrium (9d), respectively. The slack variable σ and its constraint (9e) absorb the mismatch between the nonlinear data and any LTI model. The scheme is applied in an n_z-step fashion: solve (9), apply $u_{[t,t+n_z-1]} = \hat{u}^*_{[n_z,2n_z-1]}(t)$, then set $t \leftarrow t+n_z$ and repeat. Unlike DeePC [2], (9) adds the terminal constraint (9d) and slack bound (9e) that yield the guarantees of [3].

It remains to establish that this scheme inherits the practical exponential stability of [3, Theorem 3] even though our system is nonlinear and the "noise" arises from Koopman approximation rather than measurement error. The closed-loop trajectory under the n_z-step receding-horizon application of (9) should converge to a neighborhood of (x_s, u_s) that shrinks as the embedding error vanishes.

B. Impact of Koopman Error on Data-Driven Control

Lemma 1 formalizes the noise interpretation of Section III-A quantitatively, deriving the effective noise level $\bar{\epsilon}$ in terms of the embedding quality $(\epsilon_A, \epsilon_B, \epsilon_C, c_0)$, which in turn depends on physical parameters of the system (such as sampling period and operating regime). Theorem 2 then translates this boundedness into closed-loop practical exponential stability.

Lemma 1 (Koopman Error as Bounded Output Noise)**.** *Let Φ, A, B, C, D be an approximate Koopman embedding of dimension n_z for $(\epsilon_A, \epsilon_B, \epsilon_C, c_0)$ in the sense of Definition 2, with the system operating within $\mathcal{X}$ under inputs $u \in \mathcal{U}$. Let $(u^{d,i}, y^{d,i})$ be any trajectory of the nonlinear system of length L, and define the* nominal Koopman trajectory *in deviation coordinates: $\hat{z}_0^{\text{nom},i} = \bar{z}_0^i$, $\hat{z}_{k+1}^{\text{nom},i} = A\hat{z}_k^{\text{nom},i} + B\bar{u}_k^{d,i}$, and $\bar{y}_k^{\text{nom},i} = C\hat{z}_k^{\text{nom},i} + D\bar{u}_k^{d,i}$. Let $\epsilon_k^{d,i} := \bar{y}_k^{d,i} - \bar{y}_k^{\text{nom},i}$ denote the output discrepancy at step k. Then:*

(i) Uniform bound. *Defining $\bar{e} := \epsilon_A \operatorname{diam}_z + \epsilon_B \operatorname{diam}_u + c_0$, the per-step bound is*

$$\left\|\epsilon_k^{d,i}\right\|_2 \leq \bar{\epsilon}_k := \|C\|_2\, \bar{e} \sum_{l=0}^{k-1} \|A\|_2^l + \epsilon_C \operatorname{diam}_z, \tag{10}$$

and a uniform bound over all $k \leq L-1$, as required by [3, Problem (6)], is

$$\bar{\epsilon} := \max_{0 \leq k \leq L-1} \bar{\epsilon}_k = \|C\|_2\, \bar{e} \sum_{l=0}^{L-2} \|A\|_2^l + \epsilon_C \operatorname{diam}_z. \tag{11}$$

(ii) State-dependent bound. *The output discrepancy admits the sharper, state-dependent bound*

$$\left\|\epsilon_k^{d,i}\right\|_2 \leq \sum_{l=0}^{k-1} \left\|CA^l\right\|_2 \left(\epsilon_A \left\|\bar{z}_{k-1-l}^i\right\|_2 + \epsilon_B \left\|\bar{u}_{k-1-l}^i\right\|_2 + c_0\right) + \epsilon_C \left\|\bar{z}_k^i\right\|_2. \tag{12}$$

In particular, if $\epsilon_B = \epsilon_C = 0$, this simplifies to

$$\left\|\epsilon_k^{d,i}\right\|_2 \leq \epsilon_A \sum_{l=0}^{k-1} \left\|CA^l\right\|_2 \left\|\bar{z}_{k-1-l}^i\right\|_2 + c_0 \sum_{l=0}^{k-1} \left\|CA^l\right\|_2. \tag{13}$$

The proportional term depends on the actual trajectory deviation $\left\|\bar{z}_j^i\right\|_2$ rather than the worst-case diam_z; near equilibrium, the effective noise reduces to $O(c_0)$, which can be orders of magnitude smaller than the uniform bound (11)*.*

Proof: From Definition 2 applied to the trajectory $(u^{d,i}, y^{d,i})$, $\bar{y}_k^{d,i} = C\bar{z}_k^{d,i} + D\bar{u}_k^{d,i} + \eta_k^i$ with $\left\|\eta_k^i\right\|_2 \leq \epsilon_C \left\|\bar{z}_k^i\right\|_2$. The discrepancy is

$$\epsilon_k^{d,i} = C \underbrace{\left(\bar{z}_k^i - \hat{z}_k^{\text{nom},i}\right)}_{=:\,\Delta_k^i} + \eta_k^i. \tag{14}$$

The actual lifted deviation satisfies $\bar{z}_{k+1}^i = A\bar{z}_k^i + B\bar{u}_k^{d,i} + e_k^i$, while the nominal satisfies $\hat{z}_{k+1}^{\text{nom},i} = A\hat{z}_k^{\text{nom},i} + B\bar{u}_k^{d,i}$. Subtracting gives $\Delta_{k+1}^i = A\Delta_k^i + e_k^i$ with $\Delta_0^i = 0$, which unrolls to $\Delta_k^i = \sum_{j=0}^{k-1} A^{k-1-j} e_j^i$. **(i)** Taking norms via $\|A\|_2^{k-1-j}$ and using $\left\|e_j^i\right\|_2 \leq \bar{e}$ (since $x_j^i \in \mathcal{X}$, $u_j^{d,i} \in \mathcal{U}$) gives (10); the maximum over k yields (11). **(ii)** Bounding $\left\|C\Delta_k^i\right\|_2 \leq \sum_{j=0}^{k-1} \left\|CA^{k-1-j}\right\|_2 \left\|e_j^i\right\|_2$ and substituting the proportional bound from Definition 2 (without invoking diam_z) gives (12). ∎

Theorem 2 (Stability of Data-Driven MPC under Approximate Koopman Embedding)**.** *Consider a nonlinear system* (1) *admitting an approximate Koopman embedding of dimension n_z with parameters $(\epsilon_A, \epsilon_B, \epsilon_C, c_0)$ satisfying Assumption 1,*

and let $\bar{\epsilon}$ be the effective noise level from Lemma 1. Assume that the lifted pair (A, B) is controllable. Suppose:

(a) The offline input u^d is PE of order $L + 2n_z$,
(b) The prediction horizon satisfies $L \geq 2n_z$,
(c) The quantity $c_{\mathrm{pe}}\,\bar{\epsilon}$ is sufficiently small, where $c_{\mathrm{pe}} := \left\|H_{ux}^{\dagger}\right\|_2^2$ with $H_{ux} := \mathrm{col}(\mathcal{H}_{L+n_z}(u^d),\, x^d_{[0,T_{\mathrm{data}}-L-n_z]})$ and $H_{ux}^{\dagger} := H_{ux}^{\top}(H_{ux}H_{ux}^{\top})^{-1}$, with x^d the state sequence in some minimal realization of (u^d, y^d).

Then, for any $V_{\mathrm{ROA}} > 0$ such that $\{x : \|x - x_s\|_2^2 \leq V_{\mathrm{ROA}}\} \subseteq \mathcal{X}$, there exist bounds $\underline{\lambda}_\alpha, \overline{\lambda}_\alpha, \underline{\lambda}_\sigma, \overline{\lambda}_\sigma > 0$ (depending on V_{ROA}, Q, R, and $\bar{\epsilon}$) such that, for any choice of $\lambda_\alpha \in [\underline{\lambda}_\alpha, \overline{\lambda}_\alpha]$ and $\lambda_\sigma \in [\underline{\lambda}_\sigma, \overline{\lambda}_\sigma]$ (explicit bounds in [3, Eqs. (28)–(29)]), the MPC scheme (9) *is **practically exponentially stable**: there exist constants $c > 0$ and $\rho \in (0, 1)$ such that, for all initial states with $V_0 := \|x_0 - x_s\|_2^2 \leq V_{\mathrm{ROA}}$:*

$$\|x_k - x_s\|_2 \leq c\,\rho^k\,\|x_0 - x_s\|_2 + \beta(\bar{\epsilon}), \quad \forall\, k \geq 0 \tag{15}$$

where $\beta : \mathbb{R}_{\geq 0} \to \mathbb{R}_{\geq 0}$ is continuous with $\beta(0) = 0$. The constants c, ρ, and β depend on the cost matrices Q, R, the regularization parameters λ_α, λ_σ, and the system dimensions. If $\bar{\epsilon} = 0$ (exact Koopman embedding), then $\beta(\bar{\epsilon}) = 0$ and (15) *reduces to exponential stability.*

Proof: By Lemma 1, the nonlinear I/O data decompose as $(u^d, y^{d,\mathrm{nom}} + \epsilon^d)$ with $\left\|\epsilon_k^d\right\|_\infty \leq \bar{\epsilon}$, where $y^{d,\mathrm{nom}}$ are trajectories of the nominal Koopman LTI system. Under the sliding-window regime of Section III, condition (a) implies lifted excitation of order $L + n_z$ on the resulting library [15, Sec. III.B]; [15, Thm. 3] then supplies the data-driven representation of length-$(L + n_z)$ trajectories of the nominal Koopman system, which is the multi-trajectory analog of [3, Thm. 1]. The same condition (a) supplies the full row rank of H_{ux} via [3, Cor. 2], while condition (b) is [3, Assum. 4] and condition (c) is the robust stability margin condition of [3, Thm. 3]. Applying [3, Thm. 3] to the nominal Koopman LTI system with lifted region-of-attraction size $L_\Phi^2\,V_{\mathrm{ROA}}$ (so that $V_0 \leq V_{\mathrm{ROA}}$ implies $\|\bar{z}_0\|_2^2 \leq L_\Phi^2\,V_{\mathrm{ROA}}$ by the upper Lipschitz bound of Assumption 1) yields $\|\bar{z}_k\|_2 \leq \tilde{c}\,\rho^k\,\|\bar{z}_0\|_2 + \tilde{\beta}(\bar{\epsilon})$ on the lifted state. By the lower Lipschitz bound of Assumption 1, this gives (15) with $c := \tilde{c}\,L_\Phi/\ell_\Phi$ and $\beta := \tilde{\beta}/\ell_\Phi$. ∎

Since the minimal-realization state is not directly available from input–output data, c_{pe} is an analytical quantity (not computed by the controller) and condition (c) is to be read as an existence-type assumption; in practice, $\Phi(x^d)$ serves as a non-minimal surrogate that upper-bounds c_{pe}.

Remark 2. The existence of an approximate Koopman embedding suffices for the qualitative stability conclusion, whereas tightening the quantitative margin and the slack tolerance $\bar{\epsilon}$ require knowledge of the constants $(\epsilon_A, \epsilon_B, \epsilon_C, c_0)$ and the spectral properties of A and C. The systematic discovery of such embeddings is beyond the scope of this paper.

C. Tighter Bounds via Proportional Error Structure

The uniform bound $\bar{\epsilon}$ in Lemma 1(i) can be conservative in two ways: (i) it uses $\|A\|_2^l$ (spectral norm raised to a power) rather than the tighter $\left\|A^l\right\|_2$, and (ii) it replaces the state-dependent residual $\left\|\bar{z}_j^i\right\|_2$ by the worst-case diam_z. We now address the first; the second is already addressed by part (ii) of Lemma 1.

Lemma 3 (Tighter Uniform Bound)**.** *Under the same conditions as Lemma 1, the per-step output discrepancy satisfies:*

$$\bar{\epsilon}_k^{\mathrm{tight}} := \bar{e} \sum_{l=0}^{k-1} \left\|CA^l\right\|_2 + \epsilon_C\,\mathrm{diam}_z \tag{16}$$

with uniform bound $\bar{\epsilon}^{\mathrm{tight}} := \max_{0\leq k\leq L-1} \bar{\epsilon}_k^{\mathrm{tight}} = \bar{e}\sum_{l=0}^{L-2}\left\|CA^l\right\|_2 + \epsilon_C\,\mathrm{diam}_z$. This satisfies $\bar{\epsilon}^{\mathrm{tight}} \leq \bar{\epsilon}$, with strict inequality whenever A is non-normal.

Proof: Since $\Delta_k^i = \sum_{j=0}^{k-1} A^{k-1-j} e_j^i$ (from the proof of Lemma 1), applying (14):

$$\begin{aligned}\left\|C\Delta_k^i\right\|_2 &= \left\|\sum_{j=0}^{k-1} CA^{k-1-j}\,e_j^i\right\|_2 \\ &\leq \sum_{j=0}^{k-1}\left\|CA^{k-1-j}\right\|_2\left\|e_j^i\right\|_2 \leq \bar{e}\sum_{l=0}^{k-1}\left\|CA^l\right\|_2.\end{aligned}$$

∎

When A is non-normal, $\left\|A^k\right\|_2$ may grow much more slowly than $\|A\|_2^k$, so the gap between $\bar{\epsilon}^{\mathrm{tight}}$ and $\bar{\epsilon}$ can be substantial; a quantitative illustration for the synchronous generator is given in Section IV. The more significant improvement comes from preserving the proportional error structure through the entire bound, which is precisely what part (ii) of Lemma 1 achieves.

Theorem 4 (Tighter Stability via Proportional Error)**.** *Consider the setting of Theorem 2, and suppose additionally that $\epsilon_B = \epsilon_C = 0$. Define:*

$$S_L := \sum_{l=0}^{L-2}\left\|CA^l\right\|_2 \tag{17}$$

and the offset-only noise level $\bar{\epsilon}_0 := c_0\,S_L$. Let L_Φ be the upper Lipschitz constant from Definition 2. Then:

*(a) **(Conditional bound)** For any $r > 0$, if $\|x_k - x_s\|_2 \leq r/L_\Phi$ for all k in the offline and online trajectories, the effective noise level can be tightened from $\bar{\epsilon}$ to:*

$$\bar{\epsilon}(r) := \epsilon_A\,S_L\,r + \bar{\epsilon}_0. \tag{18}$$

*(b) **(Fixed-point argument)** Provided $\epsilon_A\,S_L$ is sufficiently small, the bound* (15) *from Theorem 2 holds with $\bar{\epsilon}$ replaced by $\bar{\epsilon}(r^*)$, where r^* is the smallest positive solution of:*

$$r = L_\Phi\big(c\,\|x_0 - x_s\|_2 + \beta(\bar{\epsilon}(r))\big), \tag{19}$$

with c, β from Theorem 2. Since β is continuous with $\beta(0) = 0$ and $\bar{\epsilon}(r) \to \bar{\epsilon}_0 = O(c_0)$ as $r \to 0$, the fixed-point r^* exists and yields:

$$\limsup_{k\to\infty}\|x_k - x_s\|_2 \leq \beta\big(c_0\,S_L\big) \tag{20}$$

which depends on c_0 (the offset) rather than $\epsilon_A\,\mathrm{diam}_z$ (the worst-case proportional error).

Proof: **Part (a).** If $\|x_k - x_s\|_2 \leq r/L_\Phi$, then by Lipschitz continuity, $\|\bar{z}_k\|_2 = \|\Phi(x_k) - \Phi(x_s)\|_2 \leq L_\Phi\,\|x_k - x_s\|_2 \leq r$ for all k. Lemma 1(ii) with $\epsilon_B = \epsilon_C = 0$ then gives

$\left\|\epsilon_k^{d,i}\right\|_2 \le \epsilon_A S_L r + c_0 S_L = \bar{\epsilon}(r)$. This is a valid uniform noise bound, so Theorem 2 applies with $\bar{\epsilon}$ replaced by $\bar{\epsilon}(r)$.

Part (b). The bound (15) with noise level $\bar{\epsilon}(r)$ gives $\|x_k - x_s\|_2 \le c\|x_0 - x_s\|_2 + \beta(\bar{\epsilon}(r))$ for all k (taking the maximum of the right-hand side over k). The hypothesis of part (a), $\|x_k - x_s\|_2 \le r/L_\Phi$, holds throughout the closed loop if and only if $r \ge L_\Phi(c\|x_0 - x_s\|_2 + \beta(\bar{\epsilon}(r)))$. The smallest such r is the fixed point r^* of (19). This fixed point exists when $\epsilon_A S_L$ is sufficiently small (so that $\beta(\bar{\epsilon}(\cdot))$ grows slowly enough as a function of r). The asymptotic tracking error is $\limsup_k \|x_k - x_s\|_2 \le \beta(\bar{\epsilon}(r^*)) \le \beta(\bar{\epsilon}_0) = \beta(c_0 S_L)$. ■

Remark 3 (Improvement over Theorem 2)**.** Theorem 4 gives an asymptotic error $\beta(c_0 S_L)$ versus $\beta(\bar{\epsilon})$ from Theorem 2. The improvement has two sources: (i) $S_L = \sum \left\|CA^l\right\|_2$ is tighter than $\|C\|_2 \sum \|A\|_2^l$ (Lemma 3); and (ii) the proportional structure replaces $\bar{e} = \epsilon_A \operatorname{diam}_z + c_0$ by c_0 alone. The second effect dominates when $c_0 \ll \epsilon_A \operatorname{diam}_z$, which is generic near an equilibrium. Since $\beta = O(\bar{\epsilon}^2)$ for small $\bar{\epsilon}$ [3], this effectively eliminates ϵ_A from the asymptotic bound, leaving only c_0 (illustrated for the generator in Section IV).

IV. Application to the Synchronous Generator

We now apply the framework developed in Sections II–III to the synchronous generator model. This section serves both to make the assumptions of Theorems 2 and 4 concrete on a physically meaningful example, and to provide quantitative bounds illustrating the conservatism analysis of Section III-C.

A. Synchronous Generator Model

We consider a single synchronous generator connected to an infinite bus, modeled by the classical flux-decay model without exciter or governor dynamics. The state is $x = (\delta, \omega, E'_q)^\top \in \mathbb{R}^3$, where δ is the rotor angle, ω the rotor angular velocity, and E'_q the q-axis transient internal voltage. The control input is $u_k = T_M \in \mathbb{R}$ (mechanical torque). With sampling period $\Delta t > 0$ and Euler discretization, the system takes the form (1) with $f : \mathbb{R}^3 \times \mathbb{R} \to \mathbb{R}^3$ given component-wise by:

$$\delta_{k+1} = \delta_k + \Delta t(\omega_k - \omega_s) \tag{21}$$

$$\omega_{k+1} = \omega_k + \frac{\Delta t}{M}\left[T_M - D(\omega_k - \omega_s) - \frac{E'_{q,k} V_\infty}{X_\Sigma}\sin\delta_k\right] \tag{22}$$

$$E'_{q,k+1} = E'_{q,k} + \frac{\Delta t}{T'_{d0}}\left[E_{fd} - \frac{X_d + X_e}{X_\Sigma}E'_{q,k} + \frac{(X_d - X'_d)V_\infty}{X_\Sigma}\cos\delta_k\right]. \tag{23}$$

Here, ω_s is the synchronous speed, $M := 2H/\omega_s$ the normalized inertia, D the damping, T'_{d0} the d-axis transient time constant, X_d, X'_d, X_e the synchronous, transient, and line reactances, $X_\Sigma := X'_d + X_e$, V_∞ the bus voltage, and E_{fd} the field voltage. The nonlinearities are trigonometric ($\sin\delta, \cos\delta$) and bilinear ($E'_q \sin\delta$); the input $u = T_M$ enters affinely through (22). The system has $n = 3$ states, $m = 1$ input, and $p = 2$ outputs $y_k = (\tilde{\omega}_k,\ P_{e,k})^\top$, where $\tilde{\omega}_k := \omega_k - \omega_s$ and $P_{e,k} = \frac{E'_{q,k} V_\infty}{X_\Sigma}\sin\delta_k$.

For this application, the operating region of Section II is $\mathcal{X} := \{(\delta, \omega, E'_q) : |\delta - \delta_s| \le \delta_{\max},\ |\omega - \omega_s| \le \omega_{\max},\ E'_{q,\min} \le E'_q \le E'_{q,\max}\}$, with δ_s the pre-fault equilibrium angle, $\delta_{\max} < \pi/2$, and $\omega_{\max} \ll \omega_s$; the input set is $\mathcal{U} := [T_{M,\min}, T_{M,\max}]$. The per-step angle change then satisfies $|\Delta t(\omega_k - \omega_s)| \le \Delta t\,\omega_{\max} \ll 1$ for typical rates ($\Delta t \le 0.005$ s), as exploited below.

B. Approximate Koopman Embedding for the Generator

Theorem 5. *Consider the discretized generator* (21)–(23) *operating within the compact domain $\mathcal{X}$ and input set $\mathcal{U}$ defined above. Define the lifting:*

$$\Phi(x) = \operatorname{col}(\delta,\ \tilde{\omega},\ E'_q,\ \sin\delta,\ \cos\delta,\ E'_q\sin\delta,\ E'_q\cos\delta) \tag{24}$$

Then, $z_k = \Phi(x_k)$ satisfies an approximate Koopman linear embedding (Definition 2) of dimension $n_z = 7$ centered at the equilibrium (x_s, u_s) with

$$\epsilon_A = \kappa_A\,\Delta t, \quad \epsilon_B = 0, \quad \epsilon_C = 0, \tag{25}$$

$$c_0 = \kappa_0\,(\Delta t\,\omega_{\max})^2, \tag{26}$$

where $\kappa_A > 0$ depends on T'_{d0}, X_d, X'_d, V_∞, X_Σ, $E'_{q,\max}$, E_{fd}, and $\kappa_0 := 2 + 2E'_{q,\max}$ (see [20] for the explicit expression of κ_A). The bound is proportional with offset:

$$\|e_k\|_2 \le \epsilon_A\ \|\Phi(x_k) - \Phi(x_s)\|_2 + c_0. \tag{27}$$

Proof: See the extended arXiv version [20]. ■

As shown in Appendix I of [20], the proportional constant $\epsilon_A = O(\Delta t)$ receives contributions from the trigonometric propagation in components 4–5 and the bilinear products $E'_q\sin\delta, E'_q\cos\delta$ in components 6–7. The offset c_0 arises from the Taylor remainders in the small-angle approximation, with $\Delta t\,\omega_{\max}$ being the per-step angle deviation bound from the operating-region. For typical generator parameters ($\Delta t = 0.0025$ s, $T'_{d0} \approx 6$ s, $\omega_{\max} = 0.02$ pu): $\epsilon_A \approx 0.015$ and $c_0 \approx 10^{-8}$, so the offset is negligible relative to ϵ_A, with $c_0/\epsilon_A \approx 7 \times 10^{-7}$ pu.

Remark 4 (Non-Controllability and Non-Observability of the Embedding)**.** The raw $n_z = 7$ realization (A, B) in (2) with $B = (0, \frac{\Delta t}{M}, 0, 0, 0, 0, 0)^\top$ is *not* controllable: $\mathcal{C}(A, B) := [B,\ AB,\ \ldots,\ A^{n_z-1}B]$ has rank 2, spanning only $\{z_1, z_2\} = \{\delta, \tilde{\omega}\}$, since the coupling of components 3–7 to z_1, z_2 resides in the residual e_k, not in A; likewise (C, A) is not observable. The controllability hypothesis of Theorem 2 is nonetheless met, as it applies to a *minimal* realization of $G(z) = C(zI - A)^{-1}B + D$, of order $n_{\text{eff}} \le n_z$, which is controllable and observable by construction.

C. Conservatism of the Uniform Bound and Recovery via Proportional Structure

Theorem 2, applied to the generator with the constants from Theorem 5, gives an effective noise level $\bar{\epsilon} = \|C\|_2\,\bar{e}\sum_{l=0}^{L-2}\|A\|_2^l$ with $\bar{e} = \epsilon_A \operatorname{diam}_z + c_0$. While each factor is individually moderate, the product can be large. For the minimum horizon $L = 14$ with typical parameters ($\Delta t = 0.0025$ s, $\omega_{\max} = 0.02$ pu, $\operatorname{diam}_z \approx 1$):

$$\bar{\epsilon} \approx \underbrace{2.5}_{\|C\|_2} \times \underbrace{0.015}_{\bar{e}} \times \underbrace{43}_{\sum\|A\|_2^l} \approx 1.6.$$

This effective noise, while $O(\Delta t)$ in scaling, has a large constant ($\|C\|_2 \sum \|A\|_2^l \approx 107$) from the accumulation of errors over L steps and the non-normality of A ($\|A\|_2 = 1.18$,

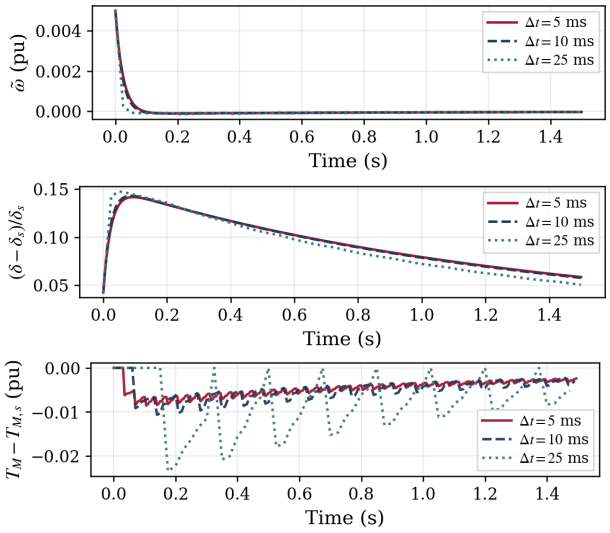

Fig. 1. Closed-loop response of (9) for the SMIB generator: speed deviation (top), normalized rotor angle deviation (middle), and control input (bottom), for $\boldsymbol{\Delta t} \in \{\mathbf{5, 10, 25}\}$ ms at fixed physical horizon $\boldsymbol{L\Delta t = 500}$ ms.

$\rho(A) = 1$). Substituted into [3, Thm. 3], $\bar{\epsilon} \approx 1.6$ yields a bound on the order of 10^3 pu, far exceeding any operationally relevant deviation, though the theorem remains qualitatively correct ($\beta(\bar{\epsilon}) \to 0$ as $\bar{\epsilon} \to 0$).

The two refinements of Section III-C resolve this. First, $\|A^k\|_2$ grows linearly in k, not exponentially as $\|A\|_2^k$ suggests: for $L = 14$, $\|C\|_2 \sum_{l=0}^{12} \|A\|_2^l \approx 107$ while $\sum_{l=0}^{12} \|CA^l\|_2 \approx 49$ (factor ~ 2); for $L = 50$ the ratio exceeds $130\times$, so Lemma 3 is essential at longer horizons. Second, applying Theorem 4 ($\epsilon_B = \epsilon_C = 0$):

$$\frac{c_0}{\bar{\epsilon}} = \frac{c_0}{\epsilon_A \operatorname{diam}_z + c_0} \approx \frac{10^{-8}}{0.015} \approx 7 \times 10^{-7}.$$

The effective noise at the equilibrium is six orders of magnitude below the worst case; since $\beta = O(\bar{\epsilon}^2)$ [3], the asymptotic error improves by $O(10^{-12})$, recovering a physically meaningful bound.

D. Closed-Loop Simulation

Closing the loop with $T_{M,s} = 0.3$ pu ($\delta_s = 27°$), we implement (9) with $n_z = 7$, $\bar{\epsilon} = 0.1$, $Q = \operatorname{diag}(10^6, 100)$, $R = 0.1$, $\lambda_\alpha = 1$, $\lambda_\sigma = 10$, and an offline library of length $10L$ excited by zero-mean $\mathcal{N}(0, 0.02^2)$ inputs. From initial state $(\delta_s + 0.02, \omega_s + 0.005\omega_s, E'_{q,s})$ with $L\Delta t = 500$ ms fixed across $\Delta t \in \{5, 10, 25\}$ ms, Fig. 1 shows the MPC drives the speed deviation to zero within ~ 0.1 s and the rotor angle monotonically to equilibrium, validating Theorem 2. The trajectories are nearly Δt-independent at fixed physical horizon, indicating the asymptotic neighborhood is dominated by c_0 rather than $\bar{\epsilon}$ (cf. Theorem 4).

V. Conclusion

We have established conditions under which data-driven MPC applied directly to input–output data from a nonlinear system yields practical exponential stability. The key insight is that an approximate Koopman embedding serves as a purely analytical certificate: the controller never uses the Koopman model, but the embedding's existence allows the nonlinear data to be interpreted as noisy LTI data, enabling the robust stability theory of [3]. The proportional error structure (Theorem 4) further recovers an asymptotic tracking error depending only on the irreducible offset c_0, which is negligible for the synchronous generator at practical sampling rates.

References

[1] J. C. Willems, P. Rapisarda, I. Markovsky, and B. L. M. De Moor, "A note on persistency of excitation," *Systems & Control Letters*, vol. 54, no. 4, pp. 325–329, 2005.

[2] J. Coulson, J. Lygeros, and F. Dörfler, "Data-enabled predictive control: In the shallows of the DeePC," in *Proc. 18th European Control Conference (ECC)*, 2019, pp. 307–312.

[3] J. Berberich, J. Köhler, M. A. Müller, and F. Allgöwer, "Data-driven model predictive control with stability and robustness guarantees," *IEEE Trans. on Automatic Control*, vol. 66, no. 4, pp. 1702–1717, 2021.

[4] C. De Persis and P. Tesi, "Formulas for data-driven control: Stabilization, optimality, and robustness," *IEEE Trans. on Automatic Control*, vol. 65, no. 3, pp. 909–924, 2020.

[5] H. J. van Waarde, J. Eising, H. L. Trentelman, and M. K. Camlibel, "Data informativity: A new perspective on data-driven analysis and control," *IEEE Trans. on Automatic Control*, vol. 65, no. 11, pp. 4753–4768, 2020.

[6] F. Dörfler, J. Coulson, and I. Markovsky, "Bridging direct and indirect data-driven control formulations via regularizations and relaxations," *IEEE Trans. on Automatic Control*, vol. 68, no. 2, pp. 883–897, 2023.

[7] I. Markovsky, "Data-driven simulation of generalized bilinear systems via linear time-invariant embedding," *IEEE Trans. on Automatic Control*, vol. 68, no. 2, pp. 1101–1106, 2023.

[8] M. Guo, C. De Persis, and P. Tesi, "Data-driven stabilization of nonlinear polynomial systems with noisy data," *IEEE Trans. on Automatic Control*, vol. 67, no. 8, pp. 4210–4217, 2022.

[9] M. Alsalti, V. G. Lopez, J. Berberich, F. Allgöwer, and M. A. Müller, "Data-based control of feedback linearizable systems," *IEEE Trans. on Automatic Control*, vol. 68, no. 11, pp. 7014–7021, 2023.

[10] J. Berberich, J. Köhler, M. A. Müller, and F. Allgöwer, "Linear tracking MPC for nonlinear systems—Part II: The data-driven case," *IEEE Trans. on Automatic Control*, vol. 67, no. 9, pp. 4406–4421, 2022.

[11] B. O. Koopman, "Hamiltonian systems and transformation in Hilbert space," *Proceedings of the National Academy of Sciences*, vol. 17, no. 5, pp. 315–318, 1931.

[12] M. Korda and I. Mezić, "Linear predictors for nonlinear dynamical systems: Koopman operator meets model predictive control," *Automatica*, vol. 93, pp. 149–160, 2018.

[13] L. Bold, M. Schaller, I. Schimperna, and K. Worthmann, "Kernel EDMD for data-driven nonlinear Koopman MPC with stability guarantees," *IFAC-PapersOnLine*, 2025, to appear.

[14] I. Schimperna, L. Bold, J. Köhler, K. Worthmann, and L. Magni, "Stability of data-driven Koopman MPC with terminal conditions," *arXiv preprint arXiv:2511.21248*, 2025.

[15] X. Shang, J. Cortés, and Y. Zheng, "Willems' fundamental lemma for nonlinear systems with Koopman linear embedding," *IEEE Control Systems Letters*, vol. 8, pp. 3135–3140, 2024.

[16] R. Strässer, M. Schaller, K. Worthmann, J. Berberich, and F. Allgöwer, "SafEDMD: A Koopman-based data-driven controller design framework for nonlinear dynamical systems," *Automatica*, vol. 185, p. 112732, 2026.

[17] L. Bold, L. Grüne, M. Schaller, and K. Worthmann, "Data-driven MPC with stability guarantees using extended dynamic mode decomposition," *IEEE Transactions on Automatic Control*, vol. 70, no. 1, pp. 534–541, 2025.

[18] L. Bold, F. M. Philipp, M. Schaller, and K. Worthmann, "Kernel-based Koopman approximants for control: Flexible sampling, error analysis, and stability," *SIAM Journal on Control and Optimization*, vol. 63, no. 6, pp. 4044–4071, 2025.

[19] I. Schimperna, K. Worthmann, M. Schaller, L. Bold, and L. Magni, "Data-driven model predictive control: Asymptotic stability despite approximation errors exemplified in the Koopman framework," *arXiv preprint arXiv:2505.05951*, 2025.

[20] A. Taghieh and S. Park, "Stability guarantees for data-driven predictive control of nonlinear systems via approximate Koopman embeddings," Available: https://arxiv.org/abs/2603.17089, 2026, extended version with full proofs.